BRAIDing receptors for cell specific targeting

Hui Chen[1,2], Sung-Jin Lee[1,2], Ryan Li[1], Asmiti Sura[1], Nicholas Suen[1], Archana Dilip[1], Yan Pomogov[1], Meghah Vuppalapaty[1], Chenggang Lu[1], Yorick Post[1], and Yang Li[1,*]

[1] Surrozen Inc., 171 Oyster Point Blvd, Suite 400, South San Francisco, CA, USA

[2] HC and SJL contributed equally to this work.

[*]Correspondence: yang@surrozen.com

Abstract

Systemic toxicity is a major challenge to therapeutic development, consequently, cell-type specific targeting is highly desirable to improve on-target cell efficacy while reducing off-target toxicity. Here, we describe a cell targeting system we called BRAID (**BR**idged **A**ctivation by **I**ntra/intermolecular **D**ivision) where an active molecule is divided into two inactive or less active parts that are subsequently brought together via a bridging receptor on target cell. We tested this hypothesis using WNT/β-catenin signaling system and demonstrated that a multivalent WNT agonist molecule divided into two inactive components induced signaling specifically on hepatocytes assembled via two different epitopes on a hepatocyte receptor, βKlotho. These data provided proof-of-concept for a cell specific targeting approach and also demonstrated the feasibility of combining different signaling pathways where desirable. This approach has broad applications to other receptor systems.

Keywords: cell targeting, split, complementation, induced proximity, WNT, Frizzled, FZD, low-density lipoprotein receptor-related protein, LRP, surrogate, WNT mimetic, stem cell, organoid, βKlotho, BRAID (**BR**idged **A**ctivation by **I**ntra/intermolecular **D**ivision), SWIFT (**S**plitting of **W**NT to **I**nduce **F**unctional **T**argeting)

INTRODUCTION

Receptor mediated signaling is fundamental to cell-cell communication, regulation of cellular growth/differentiation, maintenance of tissue function/homeostasis, and regulation of injury repair. When a cell specific response is necessary, nature achieves that selectivity through various mechanisms such as cell specific receptor, ligand gradient, short range ligand, and direct cell-cell contacts. However, most ligand receptor systems have pleiotropic effects due to broad expressions of receptors on multiple cell types. While this may be important when a coordinated response in multiple cell types or tissues is needed, achieving cell specific signaling has been a major challenge for both research and therapeutic development to avoid systemic toxicity or off-target effects. In addition, it is often difficult to identify differences between normal and diseased cells for a particular signaling pathway of interest, making it challenging, if not impossible, to selectively modulate that signaling pathway either in diseased or normal cells specifically. Therefore, effective cell targeting is needed for both research and therapeutic development.

Comparing to cell targeted antagonists, cell targeted agonists are even more complex to design. In addition to cell targeting, agonists also have stringent requirements on affinity, epitope, and geometry of the molecules (Dickopf et al., 2020). Previous efforts to engineer cell selective growth factors and cytokines have employed various approaches such as the "chimeric activators" concept (Cironi et al., 2008), where a cell targeting arm ("targeting element") is attached to either the wild-type ligand or a mutated ligand with reduced affinity toward signaling receptor ("activity element"). Such an approach has been applied to several signaling pathways, such as erythropoietin (Taylor et al., 2010, Burrill et al., 2016), interferons (Cironi et al., 2008, Garcin et al., 2014), and interleukin-2 (Ghasemi et al., 2016, Lazear et al., 2017). While little selectivity could be achieved with attaching a targeting arm to a wild-type ligand, selectivity of up to 1000-fold has been reported when a mutated ligand was used (Garcin et al., 2014). The "chimeric activators" approach is based on the cooperativity concept, where mutations that weaken the affinity of a natural ligand to its receptor are selected as the "activity element". Due to the weakened affinity, the mutant "activity element" alone displays a significantly right shifted dose response curve (or lower potency) in an activity assay, on both target and non-target cells that express the signaling receptors. When the "targeting element" is tethered to the mutant "activity element", the "targeting element" helps to increase the local concentration of the mutant "activity element" on the desired target cell surface, driving engagement of signaling receptor

and subsequent intracellular signaling activation, left shifting the activity dose response curve (increase potency) on the target cell and creating a separation between target vs non-target cells. While conceptually elegant, identifying the appropriate mutations that achieve the precise reduction of affinity that could be rescued by the "targeting element" is not trivial. In some cases, while the potency could be rescued, the maximal signaling strength remains compromised, resulting in a partial agonist. In addition, the selectivity is not exquisite, with most literature examples reporting a modest 10-fold separation between targeting vs non-targeting cells. Additional strategies have also been reported that show promising results, for example, inactive pro-drug requiring tumor-associated proteases to activate (Puskas et al., 2011, Skrombolas et al., 2019), complementation of two inactive components via targeted assembly in trans (Banaszek et al., 2019), and passive enrichment on the target cell leading to colocalization of monomeric subunits (Mock et al., 2020) or inactive "split" components (Quijano-Rubio et al., 2022).

Here, we present a novel concept to achieve cell targeting for ligand/receptor systems that involves multicomponent receptor complexes, where a productive signaling competent receptor complex formation is directly assembled through a "bridging element". We have tested this concept using the WNT/β-catenin signaling pathway as a model system.

The WNT pathway is highly conserved across species and crucial for embryonic development, and adult tissue homeostasis and regeneration (Nusse and Clevers, 2017). WNT induced signaling through β-catenin stabilization has been widely studied and is achieved by ligand binding to frizzled (FZD) and low-density lipoprotein receptor-related protein (LRP) family of receptors. There are nineteen mammalian WNTs, 10 FZDs (FZD_{1-10}), and 2 LRPs (LRP5 and LRP6). WNTs are highly hydrophobic due to lipidation that is required for function and are promiscuous, capable of binding and activating multiple FZD and LRP pairs (Janda et al., 2012, Kadowaki et al., 1996, Dijksterhuis et al., 2015). Elucidating the functions of individual FZDs in tissues has been hampered by difficulties in producing the ligands and lack of receptor and tissue selectivity. Recent breakthroughs in the development of WNT-mimetic molecules have largely resolved the production and receptor specificity challenges (Janda et al., 2017, Chen et al., 2020, Tao et al., 2019, Miao et al., 2020). While tissue selectivity could be partly achieved by tissue injury as damaged tissues seem more sensitive to WNTs (Xie et al., 2022), it still represents a significant technical and therapeutic development advancement to be able to target WNTs to specific cells and tissues.

The WNT mimetics reported so far are all bispecific and can simultaneously bind to FZDs and LRPs, and the optimal stoichiometry (at least for the antibody-based molecules) are tetravalent bispecific (2:2 format), requiring two FZD binders and two LRP binders in the same molecule to achieve efficient signaling (Tao et al., 2019, Chen et al., 2020). We took advantage of the fact that two FZD binders alone and two LRP binders alone do not signal. Cell specificity could be achieved by attaching a "targeting element" (capable of binding to another cell surface receptor, called a bridging receptor here) to these two inactive molecules, and signaling competent receptor complexes consisting of two FZDs and two LRPs could then be assembled via the bridging receptor on the target cell surface. This approach reduces or eliminates the need to mutate and reduce the affinity of the "active elements" toward signaling receptors, and creates a highly cell specific activation of the signaling pathway as the individual components are inactive. The detailed proof of concept studies based on the WNT/β-catenin signaling pathway are presented herein. We have called the cell targeted WNT mimetics SWIFT (**S**plitting of **W**NT to **I**nduce **F**unctional **T**argeting).

RESULTS

Conceptual design of cell targeted activators via a bridging receptor

Fig. 1A shows one optimized design for a WNT mimetic that is a tetravalent bispecific antibody-based molecule. It is important to highlight that efficient WNT/β-catenin signaling requires two FZD binding domains and two LRP binding domains in one molecule (Chen et al., 2020). Fig. 1B shows a cell targeting approach using the bridging receptor concept, the SWIFT approach. The first step of this concept is to split the active molecule into inactive components. In the case of the tetravalent bispecific WNT mimetic, the active molecule is split into one molecule having two FZD binding arms and a second molecule having two LRP binding arms. These two inactive components are then each tethered to a different "bridging element" binding to a different epitope on the same bridging receptor (BR, the tethered molecules named αLRP-αBR-1 and αFZD-αBR-2 in Fig. 1B, top two panels). αLRP-αBR-1 and αFZD-αBR-2 are each inactive on non-targeting cells where the bridging receptor (BR) is not expressed (Fig. 1C top panels). On targeting cells where the BR is expressed, FZD and LRP are then assembled or brought into proximity with one another by αLRP-αBR-1 and αFZD-αBR-2 via BR recreating the signaling competent receptor complexes (Fig. 1B bottom panel).

Proof of concept with the targeted WNT mimetic molecules

To test the concept shown in Fig. 1B, we selected βKlotho and endocrine fibroblast growth factor 21 (FGF21) ligand system as the bridging receptor system. FGF21 is an endocrine hormone produced by the liver that regulates metabolic homeostasis (BonDurant and Potthoff, 2018). FGF21 signals through FGFR1c, FGFR2c, and FGFR3c in the presence of co-receptor βKlotho (Zhang and Li, 2015). The binding of FGF21 to the receptor complex is primarily driven by its affinity toward βKlotho via its C-terminal domain (Lee et al., 2018, Shi et al., 2018), while its N-terminal domain is important for FGFR interaction and signaling (Yie et al., 2012, Micanovic et al., 2009). βKlotho binding antibodies have also been identified that could induce βKlotho/FGFR signaling and one particular agonistic βKlotho antibody binds to a different epitope on βKlotho from FGF21 and does not compete with FGF21 binding (Min et al., 2018). Therefore, the following bridging receptor (βKlotho) binding elements were selected to test the cell targeting SWIFT concept:

141 FGF21FL (full length FGF21) that can bind to βKlotho and competent to induce FGFR
142 signaling;
143 FGF21ΔC (FGF21 without the C-terminal βKlotho interaction domain) that does not bind
144 βKlotho nor capable of inducing FGFR signaling;
145 FGF21ΔN (FGF21 without the N-terminal FGFR interaction domain) that binds βKlotho but
146 does not signal;
147 FGF21ΔNΔC that cannot bind βKlotho and cannot signal;
148 39F7 IgG that binds βKlotho and can induce FGFR signaling.
149 The FZD and LRP binding domains selected are F (binds $FZD_{1,2,5,7,8}$) and L (binds LRP6)
150 previously named as F1 and L2, respectively (Chen et al., 2020). The graphic representations of
151 the binders and the various combinations are shown in Figs. 2A-C.
152 To test the concept in Fig. 1B, the FZD binder (F) was combined with two versions of bridging
153 receptor (βKlotho) binder, F-FGF21FL and F-FGF21ΔN (Fig. 2B), and the LRP binder (L) was
154 combined with the other bridging receptor (βKlotho) binder 39F7 as L-39F7 (Fig. 2B).
155 We first confirmed the binding of the various fusion molecules shown in Fig. 2B and 2C to their
156 respective target proteins. All F and L containing molecules bound to either FZD_7 or LRP6 E3E4
157 fragments as expected (Figs. 2D-J). FGF21FL, FGF21ΔN, and 39F7 bound to βKlotho, while
158 FGF21 without its C-terminal domain (FGF21ΔC and FGF21ΔNΔC) lost bindings to βKlotho
159 (Figs. 2D-J). Therefore, the molecule formats of the various fusion proteins had no significant
160 impact on the individual binding element's binding to their target receptors. Next, we performed
161 the Octet binding assays to assess whether the F-FGF21 or L-39F7 allow simultaneous bindings
162 to their target receptors. Sequential additions of the various F-FGF21 fusion molecules to the
163 sensor surface, followed by FZD_7 CRD, and then βKlotho show that a stepwise increase in
164 binding signal was observed with FZD_7 CRD, but only F-FGF21FL and F-FGF21ΔN showed
165 additional binding to βKlotho but not from F-FGF21ΔC or F-FGF21ΔNΔC (Fig. 2K). This
166 suggests that both F-FGF21FL or F-FGF21ΔN are capable of simultaneous bindings to both
167 FZD_7 and βKlotho receptors. Sequential additions of the various L, 39F7, and αGFP
168 combinations to the sensor surface, followed by LRP6E3E4, and then βKlotho show that a
169 stepwise increase in binding signal with L-39F7 but not the other negative control molecules,
170 αGFP-39F7 or L-αGFP (Fig. 2L). This suggests that L-39F7 can simultaneously bind to both
171 LRP6 and βKlotho receptors.

The ability of this set of molecules to activate WNT/β-catenin signaling was assessed in WNT-responsive Huh7 and HEK293 Super TOP-FLASH (STF) reporter cells (Zhang et al., 2020). As shown in Fig. 3B, the combination of F-FGF21FL or F-FGF21ΔN with L-39F7 resulted in WNT/β-catenin signaling in the liver cell line, Huh7 cells which expresses the bridging receptor βKlotho (*KLB*), but not in 293 cells where βKlotho is not expressed (Fig. 3A and 3G). This signaling depends on the presence of both FZD and LRP binding arms and the ability to bind the bridging receptor, as the removal of LRP binding arm L from L-39F7 or inactivation of βKlotho binding arms (use of FGF21ΔC or FGF21ΔNΔC, or the replacement of 39F7 with αGFP) resulted in no activity in either cells (Figs. 3A-F). This provided experimental evidence supporting the SWIFT concept presented in Fig. 1B.

Validation of liver specific targeting with primary human cells

To test the potency of these molecules in cells directly derived from the tissue of interest we selected primary human hepatocytes and human small intestinal organoids (Fig. 4A). These cultures better represent the physiological and transcriptional characteristics of the liver and intestine compared to cell lines. As expected, primary human hepatocytes express bridging receptor βKlotho, while human small intestinal cells do not (Fig. 4B). The combination of F-FGF21ΔN and L-39F7 in human hepatocytes had a robust increase in the expression of WNT target gene *AXIN2* after 24 hours compared to the control (Fig. 4C). The combination with negative control F-FGF21ΔNΔC did not result in the elevation of *AXIN2*. The same panel of molecules did not elicit any target gene expression in human small intestinal cells, confirming the need for bridging receptor expression for activity (Fig. 4D). These results in primary cells support the feasibility of cell specific targeting, and we expect them to be predictive of tissue specific *in vivo* responses.

199 **DISCUSSION**

200 A major deficiency in therapeutic development today is effective approaches to target drugs
201 toward a desired cell type. Due to the pleiotropic expression and actions of most drug targets in
202 many cell types/organs or lack of differentiation between diseased vs normal cells, many drugs
203 exhibit either dose limiting toxicity or act on multiple cell types of opposing activity that render
204 drugs less effective. Therefore, developing effective cell targeting methods would allow reduced
205 systemic toxicity and higher efficacy for more effective treatments.

206 Here we describe a novel cell targeting approach we termed BRAID where an active drug
207 molecule is divided into inactive parts that are assembled via a bridging receptor specific to the
208 target cell. Although complementation and splitting a molecule into inactive parts have been
209 explored previously, the novelty of our approach is that there is no requirement for the two split
210 inactive components to interact with one another and therefore, does not require cooperative
211 interactions between the split components and receptors for activity. The assembly of the
212 signaling complex by our approach is achieved by simultaneous binding of the two divided
213 inactive components through a common bridging receptor (Fig. 1B).

214 We tested this concept on WNT/β-catenin signaling pathway as a model system. This signaling
215 system requires two receptors, FZD and LRP. We, and others, have generated antibody based
216 WNT mimetic molecules by linking FZD binders and LRP binders into a single molecule to
217 activate the FZD/LRP receptor complex (Chen et al., 2020; Janda et al., 2017, Tao et al., 2019).
218 To explore the BRAID concept with the WNT signaling receptors, we first divided the
219 tetravalent bispecific WNT mimetic into two components: one contains two FZD binding
220 domains and the other contains two LRP binding domains. To each of these two inactive
221 components, a binding moiety to the bridging receptor, βKlotho (predominantly expressed in
222 hepatocytes), was attached. The two bridging receptor binding moieties are FGF21 and 39F7
223 which bind to non-overlapping regions on βKlotho (Min et al., 2018). As demonstrated both on
224 WNT responsive reporter cell lines as well as on primary human hepatocytes and human
225 intestinal organoids, target cell specific WNT signaling was indeed observed when the two
226 inactive components were combined. The signaling only occurred on the target cell hepatocytes,
227 but not on HEK293 nor intestinal cells. Furthermore, activity depends on the presence of
228 βKlotho binding domains on the two inactive components, as removal of βKlotho binding on
229 either the FZD or the LRP half of the molecule or having βKlotho but not LRP binding, resulted

230 in inactive combinations (Figs. 3 and 4). These results provided compelling evidence for this
231 novel cell targeting concept. We envision that other potential ways of dividing the WNT or the
232 WNT mimetic molecules, including different geometry, or stoichiometry of FZD/LRP ratios,
233 linker length, or having one each of FZD and LRP binding arms as one component may also
234 result in active targeted WNT mimetics. We have termed this cell targeted WNT system,
235 SWIFT. As WNT plays important roles in many tissues during development and in adult tissue
236 homeostasis and injury repair, and dysregulated WNT signaling may result in various human
237 diseases (Nusse and Clevers, 2017), SWIFT offers the opportunity to more specifically target
238 WNT activation in desired cell types that can help both research and therapeutic development.
239 In conclusion, we describe here a novel cell targeting approach that can be broadly applied to
240 various signaling systems. This approach also allows the combination of different signaling
241 pathways together resulting in additive or synergistic effects.
242
243

Acknowledgments: The authors would like to thank Leona Cheng, Haili Zhang, Jasmine Tan, Hayoung Go, and Sean Bell for technical support and discussions. We thank Huy Nguyen for the illustration in Figure 1. And we thank Wen-Chen Yeh and Craig Parker for critical reading of the manuscript and Kathee Littrell for editorial support.

Author contributions: HC, SJL and YP Formal analysis, Supervision, Investigation, Visualization, Methodology, Writing—review and editing; HC, SJL, RL, AS, NS, AD, YP, MV, CL and YP, Resources, Investigation, Visualization, Methodology, Writing—review and editing; YL, Conceptualization, Formal analysis, Resources, Supervision, Funding acquisition, Visualization, Methodology, Writing—original draft; Writing—review and editing

Declaration of interests: All authors are current or former full-time employees and shareholders of Surrozen, Inc. YL is Senior Vice President, Biology at Surrozen, Inc. A patent application is pending for the work described in this manuscript.

MATERIALS AND METHODS

Molecular Cloning

All constructs were cloned into pcDNA3.1(+) mammalian expression vector (Thermo Fisher). The–L-scFv binder was constructed by fusing the heavy-chain variable region (VH) to the N-terminus of the light-chain variable (VL) region with a 15-mer linker (GSAASGSSGGSSSGA); The anti-GFP scFv binder was constructed by fusing the VH to the N-terminus of the VL with a 15-mer linker (GGGGSGGGGSGGGGS). All human IgG1 constructs contain the L234A/L235A/P329G mutations (LALAPG) in Fc domain to eliminate effector function (Lo et al., 2017). For generating the constructs of scFv-39F7 IgG1**,** the scFv binder was fused to the N-terminus of 39F7 LC with a 5-mer-linker GSGSG. For generating the construct of L-αGFP IgG1**,** the L-scFv was fused to the N-terminus of αGFP LC with a 15-mer-linker GSGSGGSGSGGSSGG. For generating the FGF21-variants appended F IgG molecules, FGF21 variants were fused to the C-terminus of the LC of F IgG1 (LALAPG) with a 5-mer-linker (GGSGS). FGF21FL has the mature protein sequence (H29-S209) with RGE mutations in the C-terminus (Stanislaus et al., 2017); FGF21ΔN is the sequence of FGF21FL with the deletion of the N-terminus of sequence of H29-R45; FGF21ΔC is the sequence of FGF21FL with the deletion of the C-terminus S190-S209; FGF21ΔNΔC is the sequence of FGF21FL with the deletion of both the N-terminal sequence of H29-R45 and the C-terminal sequence of S190-S209.

Protein Production

All recombinant proteins were produced in Expi293F cells (Thermo Fisher Scientific) by transient transfection. The proteins were first purified using CaptivA Protein A affinity resin (Repligen), unless otherwise specified. All proteins were further polished with Superdex 200 Increase 10/300 GL (GE Healthcare Life Sciences) size-exclusion chromatography (SEC) using 1 x HBS buffer (20 mM HEPES pH 7.4, 150 mM NaCl). The proteins were subsequently examined by SDS-polyacrylamide electrophoresis and estimated to have > 90% purity.

Super Top-Flash (STF) Assay

WNT signaling activity was measured using HEK293 and Huh7 cells containing a luciferase gene controlled by a WNT-responsive promoter (STF assay) as previously reported Zhang et al.,

290 2020. In brief, cells were seeded at a density of 10,000 per well in 96-well plates 24 hours prior
291 to treatment at the presence of 3 μM IWP2 to inhibit the production of endogenous WNTs and
292 the presence of 20 nM Fc-Rspodin 2. Cells were lysed with Luciferase Cell Culture Lysis
293 Reagent (Promega) and luciferase activity was measured with Luciferase Assay System
294 (Promega) using vendor suggested procedures.
295
296 **Affinity Measurement and Step-Binding Assay**
297 Binding kinetics of F-FGF21 series (F-FGF21FL, F-FGF21ΔN, F-FGF21ΔC, and F-
298 FGF21ΔNΔC) to human FZD_7 CRD and βKlotho (Fisher Scientific) or L-39F7 series (L-39F7,
299 αGFP-39F7, and L-αGFP) to human LRP6E3E4 and βKlotho, respectively, were determined by
300 bio-layer interferometry (BLI) using an Octet Red 96 (PALL ForteBio) instrument at 30°C, 1000
301 rpm with AHC biosensors (Sartorius). Various F-FGF21 or L-39F7 proteins were diluted to 50
302 nM in the running buffer and captured to the AHC biosensor, followed by dipping into wells
303 containing the FZD_7 CRD, LRP6E3E4 and βKlotho at different concentrations in a running
304 buffer or into a well with only the running buffer as reference channel. The dissociation of the
305 interaction was followed with the running buffer. The monovalent K_D for each binder was
306 calculated by Octet System software, based on fitting to a 1:1 binding model.
307 Step-binding assay was performed with the BLI using the Octet Red 96 instrument at 30°C, 1000
308 rpm with AHC biosensors. Various F-FGF21 or L-39F7 proteins were diluted to 50 nM in the
309 running buffer and captured to the AHC biosensor, followed by dipping into wells containing the
310 100 nM FZD_7 CRD or 100 nM LRP6E3E4, respectively. The sensor chips next moved into 150
311 nM βKlothos containing 100 nM FZD_7 CRD or containing 100 nM LRP6E3E4 to check the
312 additional bindings of β-Klotho. Sensorgram slopes were compared for βKlotho bindings.
313
314 **Primary human cells**
315 Human hepatocytes were purchased from BioIVT (10-donor pooled cryoplateable X008001-P)
316 and cultured in LONZA hepatocyte maintenance medium (CC-3198). In short, plastic culture
317 plates were coated with 20% Matrigel Matrix (CB40230C) and cells were plated in plating
318 medium (BioIVT Z990003). After four hours the medium was changed to maintenance medium
319 and refreshed every day for three days prior to the 24h experiment.

320 Human small intestinal organoids were a gift from the Calvin Kuo Lab at Stanford. Organoids
321 were maintained and expanded as previously described (Sato et al., 2011). In short, adapted
322 expansion medium contained Advanced DMEM, 10 mM HEPES, 1x GlutaMAX, 1X Penicillin-
323 Streptomycin, 1x B27, 1x N2, 1.25 mM N-acetylcysteine, 10 mM Nicotinamide, 50 ng/mL
324 recombinant human EGF, 50 ng/mL recombinant human Noggin, 20 nM R-Spondin 2, 0.1 nM
325 L-F Wnt mimetic, 10 nM recombinant Gastrin, 500 nM A83-01 and 10 μM SB202190.
326 Treatment of molecules was done in the presence of 20 nM R-spondin 2 for 24h at a
327 concentration of 10 nM. After 24 hours the cells were harvested and RNA collected for qPCR.
328 Each experiment with both primary human hepatocytes and human small intestinal organoids
329 was repeated three times.
330
331 **Quantitative polymerase chain reaction analysis of gene expression**
332 RNAs from HEK293, Huh7 cells, or primary human cells were extracted using the Qiagen
333 RNeasy Micro Kit (Qiagen). cDNA was produced using the SuperScript IV VILO cDNA
334 Synthesis Kit (Thermo Fisher). βKlotho (*KLB*) RNA was quantified using Maxima SYBR Green
335 qPCR master mix on a Bio-Rad CFX96 real time PCR machine.
336 Cycle threshold (C_t) values were normalized to the expression of constitutive *ACTINB* RNA
337 using the following oligo's: ACTB_F1: CTGGAACGGTGAAGGTGACA. ACTB_R1:
338 AAGGGACTTCCTGTAACAATGCA. KLB_F1: ATCTAGTGGCTTGGCATGGG.
339 KLB_R1:CCAAACTTTCGAGTGAGCCTTG. KLB_F2:CACTGAATCTGTTCTTAAGCCCG.
340 KLB_R2: GGCGTTCCACACGTACAGA. KLB_F3: GGAGGTGCTGAAAGCATACCT.
341 KLB_R3: TCTCTTCAGCCAGTTTGAATGC
342
343
344

345 **Figures Legends**

346 **Figure 1**. **Diagram of the activation of the signaling pathway by the split molecules through**
347 **the binding to a bridging receptor on the targeting cell surface.** A) Efficient WNT/β-catenin
348 signaling requires two FZD binding domains and two LRP binding domains in one WNT
349 mimetic molecule. B) WNT mimetic molecule is split into one molecule having two FZD
350 binding arms (2:0) and a second molecule having two LRP binding arms (0:2) and then each
351 tethered to a different "bridging element" binding to a different epitope on the same bridging
352 receptor (named αLRP-αBR-1 and αFZD-αBR-2) (top two panels). On targeting cells where the
353 BR is expressed, FZD and LRP are then assembled by αLRP-αBR-1 and αFZD-αBR-2 via BR
354 recreating the signaling competent receptor complexes (bottom panel).

355

356 **Figure 2. Diagrams of the molecules used in the experiment to provide proof of concept for**
357 **SWIFT.** A) Elements that are used in the split molecules. LRP6 binder element is in scFv
358 format; FZD binder is in the IgG1 format; Both αGFP IgG1 and αGFP scFv are used for
359 assembly of the negative control molecules. Two types of βKlotho binders are used. Binder#1,
360 39F7 IgG1, a βKlotho monoclonal antibody; Binder#2, FGF21FL and different deletion variants.
361 B) The diagram of the assembled SWIFT molecules. C) The diagram of the assembled negative
362 control molecules. (D-G) Bindings of various F-FGF21 fusion proteins to FZD_7 and βKlotho.
363 Bindings of FZD_7 and β-Klotho to F-FGF21FL (D), F-FGF21ΔN (E), F-FGF21ΔC (F), or F-
364 FGF21ΔNΔC (G) were determined by Octet. (H-J) Binding of LRP6 and βKlotho to L-39F7 (H),
365 αGFP-39F7 (I), or L-αGFP (J) were determined by Octet. Mean K_D values were calculated from
366 all 7 binding curves with global fits (red dotted lines) using 1:1 Langmuir binding model. (K)
367 Step bindings of FZD_7 and βKlotho to various F-FGF21 fusion proteins. Sequential binding of F-
368 FGF21FL (blue sensorgram), F-FGF21ΔN (red sensorgram), F-FGF21ΔC (light green
369 sensorgram), or F-FGF21ΔNΔC (green sensorgram), followed by FZD_7 CRD, then followed by
370 addition of βKlotho on Octet shows simultaneous engagement of both FZD_7 and βKlotho to the
371 indicated F-FGF21 proteins. Sensorgrams for FZD_7 and βKlotho area (red dotted box) are
372 enlarged at the right. (L) Step binding of LRP6 and βKlotho to L-39F7 and its control proteins.
373 Sequential binding L-39F7 (blue sensorgram), L-αGFP (light blue sensorgram), αGFP-39F7 (red
374 sensorgram), or 39F7 IgG (green sensorgram), followed by LRP6E3E4, then followed by
375 addition of βKlotho on Octet shows simultaneous engagement of both LRP6 and βKlotho to the

376 indicated L-39F7 and its control proteins. Sensorgrams for LRP6 and βKlotho area (red dotted
377 box) are enlarged on the right.
378
379 **Figure 3. Dose dependent STF assay of SWIFT molecules in HEK293 and Huh7 cells.** A-F)
380 Various F-FGF21 fusion proteins in the presence of L-39F7 in HEK293 STF cells (A) and Huh7
381 STF cells (B); various F-FGF21 fusion proteins in the presence of L-αGFP in HEK293 STF cells
382 (C) and Huh7 STF cells (D); and various F-FGF21 fusion proteins in the presence of αGFP-39F7
383 in HEK293 STF cells (E) and Huh7 STF cells (F). G) Expression of bridging receptor βKlotho
384 (*KLB*) in HEK293 and Huh7 cells. Data are representative of three independent experiments
385 performed in triplicates and are shown as mean ± standard deviation (SD).
386
387 **Figure 4. Activity of targeted molecules in primary human cells.** A) Representative images of
388 primary human hepatocytes cultures in 2D or human small intestinal organoids. Scale bars 200
389 μm. B) Expression of bridging receptor βKlotho (*KLB*) in hepatocytes or small intestinal cells.
390 C) WNT target gene *AXIN2* expression normalized to control treatment after 24-hour treatment
391 with 10 nM of indicated molecules in human hepatocytes. D) WNT target gene *AXIN2*
392 expression normalized to control treatment after 24-hour treatment with 10 nM of indicated
393 molecules in human small intestinal organoids. *** = $P \leq 0.001$ (one-way ANOVA), each data
394 point represents an independent experiment performed in duplicates.
395
396
397

References

Banaszek, A., Bumm, T.G.P., Nowotny, B., Geis, M., Jacob, K., Wolfl, M., Trebing, J., Kucka, K., Kouhestani, D., Gogishvili, T., *et al.* (2019). On-target restoration of a split T cell-engaging antibody for precision immunotherapy. Nat Commun *10*, 5387.

BonDurant, L.D., and Potthoff, M.J. (2018). Fibroblast Growth Factor 21: A Versatile Regulator of Metabolic Homeostasis. Annu Rev Nutr *38*, 173-196.

Burrill, D.R., Vernet, A., Collins, J.J., Silver, P.A., and Way, J.C. (2016). Targeted erythropoietin selectively stimulates red blood cell expansion in vivo. Proc Natl Acad Sci U S A *113*, 5245-5250.

Chen, H., Lu, C., Ouyang, B., Zhang, H., Huang, Z., Bhatia, D., Lee, S.J., Shah, D., Sura, A., Yeh, W.C., *et al.* (2020). Development of Potent, Selective Surrogate WNT Molecules and Their Application in Defining Frizzled Requirements. Cell Chem Biol *27*, 598-609 e594.

Cironi, P., Swinburne, I.A., and Silver, P.A. (2008). Enhancement of cell type specificity by quantitative modulation of a chimeric ligand. J Biol Chem *283*, 8469-8476.

Dickopf, S., Georges, G.J., and Brinkmann, U. (2020). Format and geometries matter: Structure-based design defines the functionality of bispecific antibodies. Comput Struct Biotechnol J *18*, 1221-1227.

Dijksterhuis, J.P., Baljinnyam, B., Stanger, K., Sercan, H.O., Ji, Y., Andres, O., Rubin, J.S., Hannoush, R.N., and Schulte, G. (2015). Systematic mapping of WNT-FZD protein interactions reveals functional selectivity by distinct WNT-FZD pairs. J Biol Chem *290*, 6789-6798.

Garcin, G., Paul, F., Staufenbiel, M., Bordat, Y., Van der Heyden, J., Wilmes, S., Cartron, G., Apparailly, F., De Koker, S., Piehler, J., *et al.* (2014). High efficiency cell-specific targeting of cytokine activity. Nat Commun *5*, 3016.

Ghasemi, R., Lazear, E., Wang, X., Arefanian, S., Zheleznyak, A., Carreno, B.M., Higashikubo, R., Gelman, A.E., Kreisel, D., Fremont, D.H., *et al.* (2016). Selective targeting of IL-2 to NKG2D bearing cells for improved immunotherapy. Nat Commun *7*, 12878.

Janda, C.Y., Dang, L.T., You, C., Chang, J., de Lau, W., Zhong, Z.A., Yan, K.S., Marecic, O., Siepe, D., Li, X., *et al.* (2017). Surrogate Wnt agonists that phenocopy canonical Wnt and beta-catenin signalling. Nature *545*, 234-237.

Janda, C.Y., Waghray, D., Levin, A.M., Thomas, C., and Garcia, K.C. (2012). Structural basis of Wnt recognition by Frizzled. Science *337*, 59-64.

Kadowaki, T., Wilder, E., Klingensmith, J., Zachary, K., and Perrimon, N. (1996). The segment polarity gene porcupine encodes a putative multitransmembrane protein involved in Wingless processing. Genes Dev *10*, 3116-3128.

Lazear, E., Ghasemi, R., Hein, S.M., Westwick, J., Watkins, D., Fremont, D.H., and Krupnick, A.S. (2017). Targeting of IL-2 to cytotoxic lymphocytes as an improved method of cytokine-driven immunotherapy. Oncoimmunology *6*, e1265721.

Lee, S., Choi, J., Mohanty, J., Sousa, L.P., Tome, F., Pardon, E., Steyaert, J., Lemmon, M.A., Lax, I., and Schlessinger, J. (2018). Structures of beta-klotho reveal a 'zip code'-like mechanism for endocrine FGF signalling. Nature *553*, 501-505.

Lo, M., Kim, H.S., Tong, R.K., Bainbridge, T.W., Vernes, J.M., Zhang, Y., Lin, Y.L., Chung, S., Dennis, M.S., Zuchero, Y.J., *et al.* (2017). Effector-attenuating Substitutions That Maintain Antibody Stability and Reduce Toxicity in Mice. J Biol Chem *292*, 3900-3908.

Miao, Y., Ha, A., de Lau, W., Yuki, K., Santos, A.J.M., You, C., Geurts, M.H., Puschhof, J., Pleguezuelos-Manzano, C., Peng, W.C., *et al.* (2020). Next-Generation Surrogate Wnts Support Organoid Growth and Deconvolute Frizzled Pleiotropy In Vivo. Cell Stem Cell *27*, 840-851 e846.

Micanovic, R., Raches, D.W., Dunbar, J.D., Driver, D.A., Bina, H.A., Dickinson, C.D., and Kharitonenkov, A. (2009). Different roles of N- and C- termini in the functional activity of FGF21. J Cell Physiol *219*, 227-234.

Min, X., Weiszmann, J., Johnstone, S., Wang, W., Yu, X., Romanow, W., Thibault, S., Li, Y., and Wang, Z. (2018). Agonistic beta-Klotho antibody mimics fibroblast growth factor 21 (FGF21) functions. J Biol Chem *293*, 14678-14688.

Mock, J., Stringhini, M., Villa, A., Weller, M., Weiss, T., and Neri, D. (2020). An engineered 4-1BBL fusion protein with "activity on demand". Proc Natl Acad Sci U S A *117*, 31780-31788.

Nusse, R., and Clevers, H. (2017). Wnt/beta-Catenin Signaling, Disease, and Emerging Therapeutic Modalities. Cell *169*, 985-999.

Puskas, J., Skrombolas, D., Sedlacek, A., Lord, E., Sullivan, M., and Frelinger, J. (2011). Development of an attenuated interleukin-2 fusion protein that can be activated by tumour-expressed proteases. Immunology *133*, 206-220.

Quijano-Rubio, A., Bhuiyan, A.M., Yang, H., Leung, I., Bello, E., Ali, L.R., Zhangxu, K., Perkins, J., Chun, J.H., Wang, W., *et al.* (2022). A split, conditionally active mimetic of IL-2 reduces the toxicity of systemic cytokine therapy. Nat Biotechnol.

Sato, T., Stange, D.E., Ferrante, M., Vries, R.G., Van Es, J.H., Van den Brink, S., Van Houdt, W.J., Pronk, A., Van Gorp, J., Siersema, P.D., *et al.* (2011). Long-term expansion of epithelial organoids from human colon, adenoma, adenocarcinoma, and Barrett's epithelium. Gastroenterology *141*, 1762-1772.

Shi, S.Y., Lu, Y.W., Richardson, J., Min, X., Weiszmann, J., Richards, W.G., Wang, Z., Zhang, Z., Zhang, J., and Li, Y. (2018). A systematic dissection of sequence elements determining beta-Klotho and FGF interaction and signaling. Sci Rep *8*, 11045.

Skrombolas, D., Sullivan, M., and Frelinger, J.G. (2019). Development of an Interleukin-12 Fusion Protein That Is Activated by Cleavage with Matrix Metalloproteinase 9. J Interferon Cytokine Res *39*, 233-245.

Stanislaus, S., Hecht, R., Yie, J., Hager, T., Hall, M., Spahr, C., Wang, W., Weiszmann, J., Li, Y., Deng, L., *et al.* (2017). A Novel Fc-FGF21 With Improved Resistance to Proteolysis, Increased Affinity Toward beta-Klotho, and Enhanced Efficacy in Mice and Cynomolgus Monkeys. Endocrinology *158*, 1314-1327.

Tao, Y., Mis, M., Blazer, L., Ustav, M.J., Steinhart, Z., Chidiac, R., Kubarakos, E., O'Brien, S., Wang, X., Jarvik, N., *et al.* (2019). Tailored tetravalent antibodies potently and specifically activate Wnt/Frizzled pathways in cells, organoids and mice. Elife *8*.

Taylor, N.D., Way, J.C., Silver, P.A., and Cironi, P. (2010). Anti-glycophorin single-chain Fv fusion to low-affinity mutant erythropoietin improves red blood cell-lineage specificity. Protein Eng Des Sel *23*, 251-260.

Xie, L., Fletcher, R.B., Bhatia, D., Shah, D., Phipps, J., Deshmukh, S., Zhang, H., Ye, J., Lee, S., Le, L., *et al.* (2022). Robust colonic epithelial regeneration and amelioration of colitis via FZD-specific activation of Wnt signaling. Cell Mol Gastroenterol Hepatol.

Yie, J., Wang, W., Deng, L., Tam, L.T., Stevens, J., Chen, M.M., Li, Y., Xu, J., Lindberg, R., Hecht, R., *et al.* (2012). Understanding the physical interactions in the FGF21/FGFR/beta-Klotho complex: structural requirements and implications in FGF21 signaling. Chem Biol Drug Des *79*, 398-410.

Zhang, J., and Li, Y. (2015). Fibroblast Growth Factor 21 Analogs for Treating Metabolic Disorders. Front Endocrinol (Lausanne) *6*, 168.

Zhang, Z., Broderick, C., Nishimoto, M., Yamaguchi, T., Lee, S.J., Zhang, H., Chen, H., Patel, M., Ye, J., Ponce, A., *et al.* (2020). Tissue-targeted R-spondin mimetics for liver regeneration. Sci Rep *10*, 13951.

Figure 1

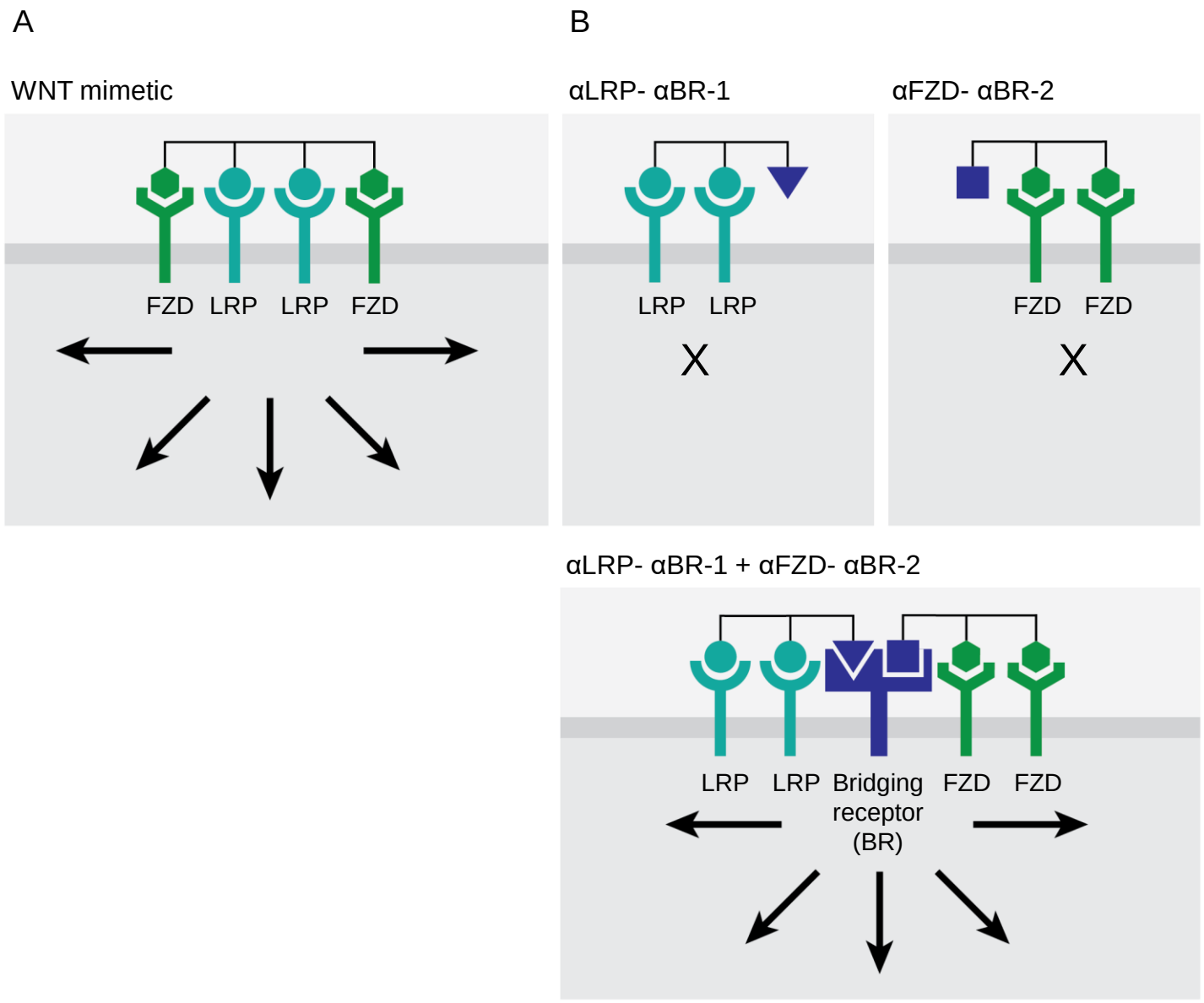
A
WNT mimetic
FZD
LRP
LRP
FZD
B
αLRP- αBR-1
LRP
LRP
X
αFZD- αBR-2
FZD
FZD
X
αLRP- αBR-1 + αFZD- αBR-2
LRP
LRP
Bridging receptor (BR)
FZD
FZD

Figure 2

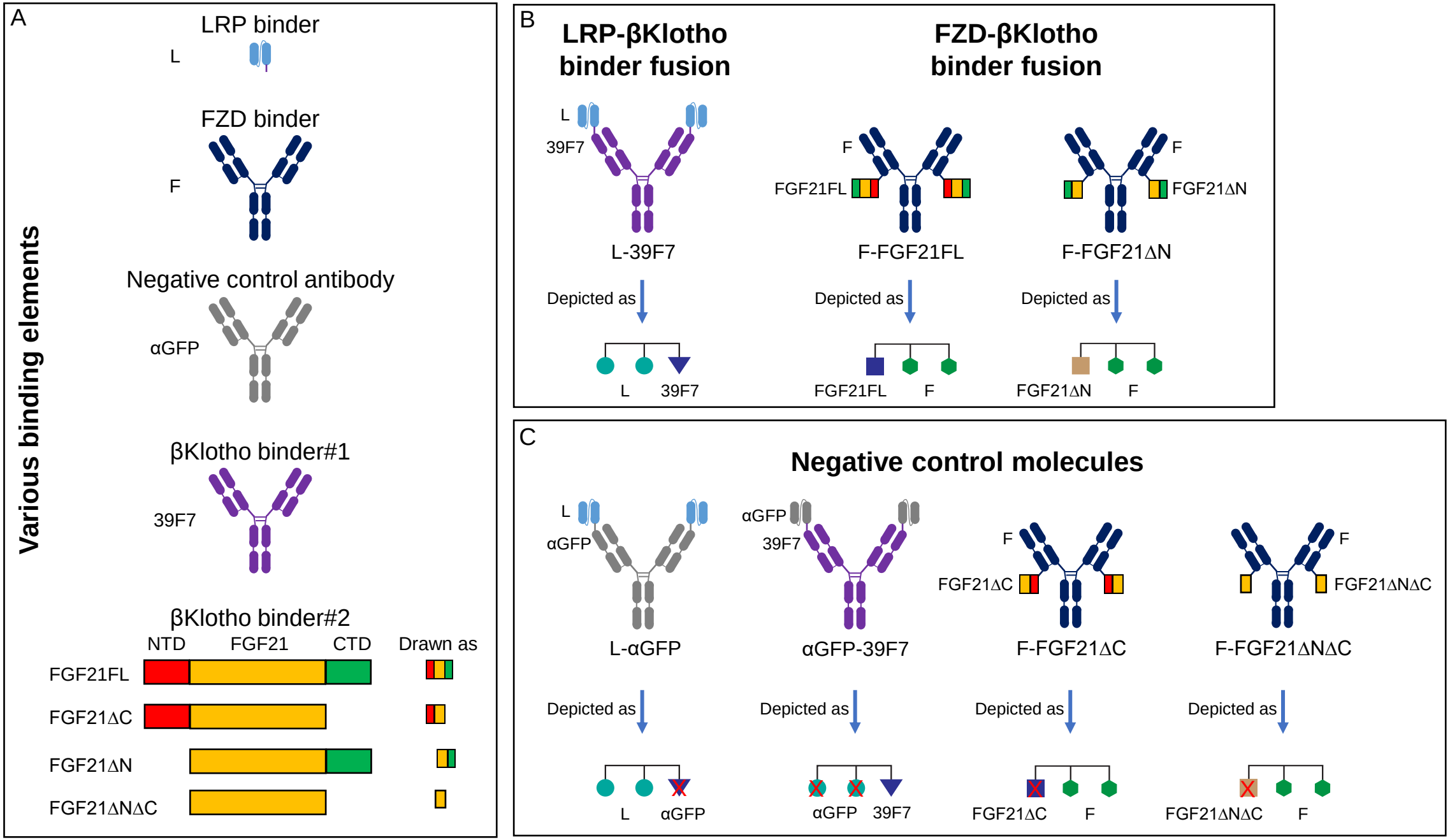
A
Various binding elements
LRP binder
L
FZD binder
F
Negative control antibody
αGFP
βKlotho binder#1
39F7
βKlotho binder#2
NTD
FGF21
CTD
Drawn as
FGF21FL
FGF21ΔC
FGF21ΔN
FGF21ΔNΔC
B
LRP-βKlotho binder fusion
FZD-βKlotho binder fusion
L
39F7
L-39F7
F
FGF21FL
F-FGF21FL
F
FGF21ΔN
F-FGF21ΔN
Depicted as
L
39F7
FGF21FL
F
FGF21ΔN
F
C
Negative control molecules
L
αGFP
L-αGFP
αGFP
39F7
αGFP-39F7
F
FGF21ΔC
F-FGF21ΔC
F
FGF21ΔNΔC
F-FGF21ΔNΔC
Depicted as
L
αGFP
αGFP
39F7
FGF21ΔC
F
FGF21ΔNΔC
F

Figure 2

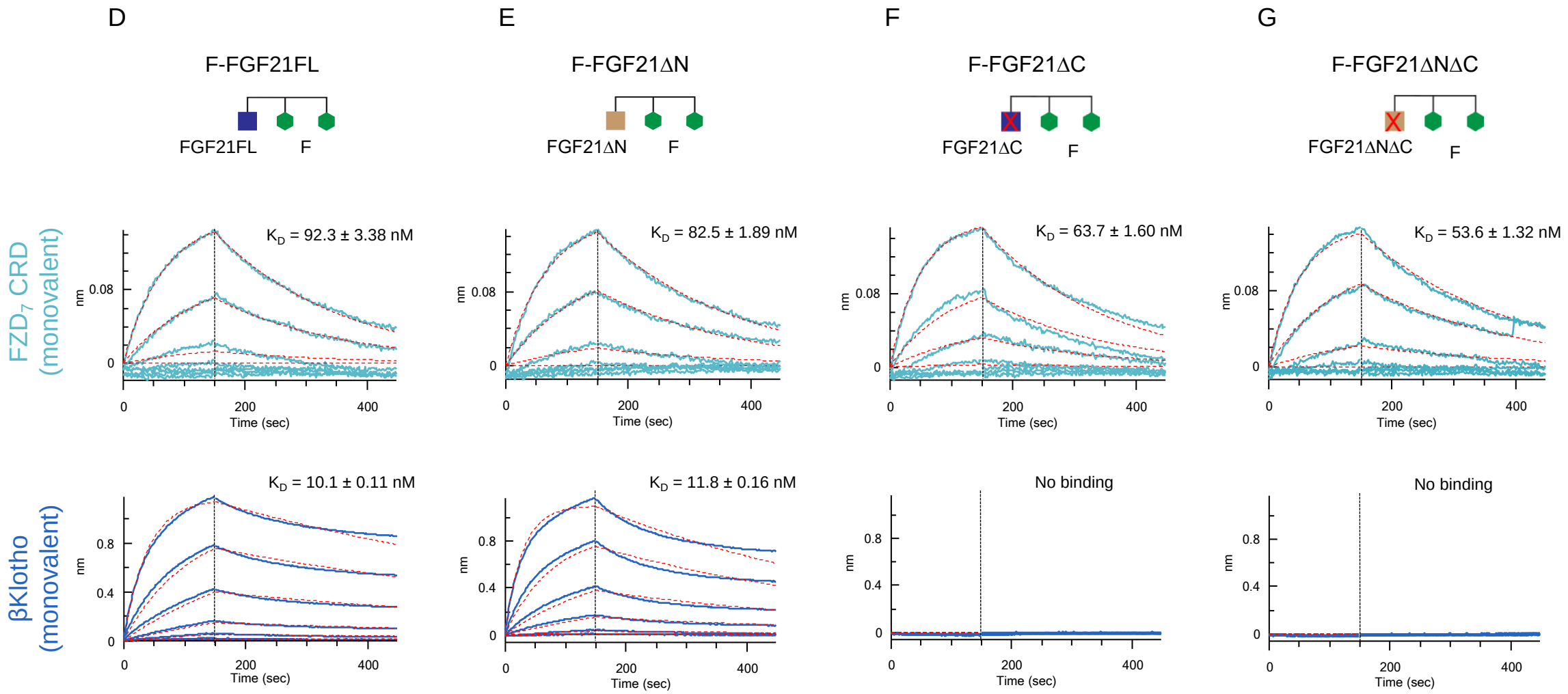
D
F-FGF21FL
FGF21FL
F
E
F-FGF21ΔN
FGF21ΔN
F
F
F-FGF21ΔC
FGF21ΔC
F
G
F-FGF21ΔNΔC
FGF21ΔNΔC
F
FZD7 CRD (monovalent)
βKlotho (monovalent)
nm
Time (sec)
KD = 92.3 ± 3.38 nM
KD = 82.5 ± 1.89 nM
KD = 63.7 ± 1.60 nM
KD = 53.6 ± 1.32 nM
KD = 10.1 ± 0.11 nM
KD = 11.8 ± 0.16 nM
No binding
No binding

Figure 2

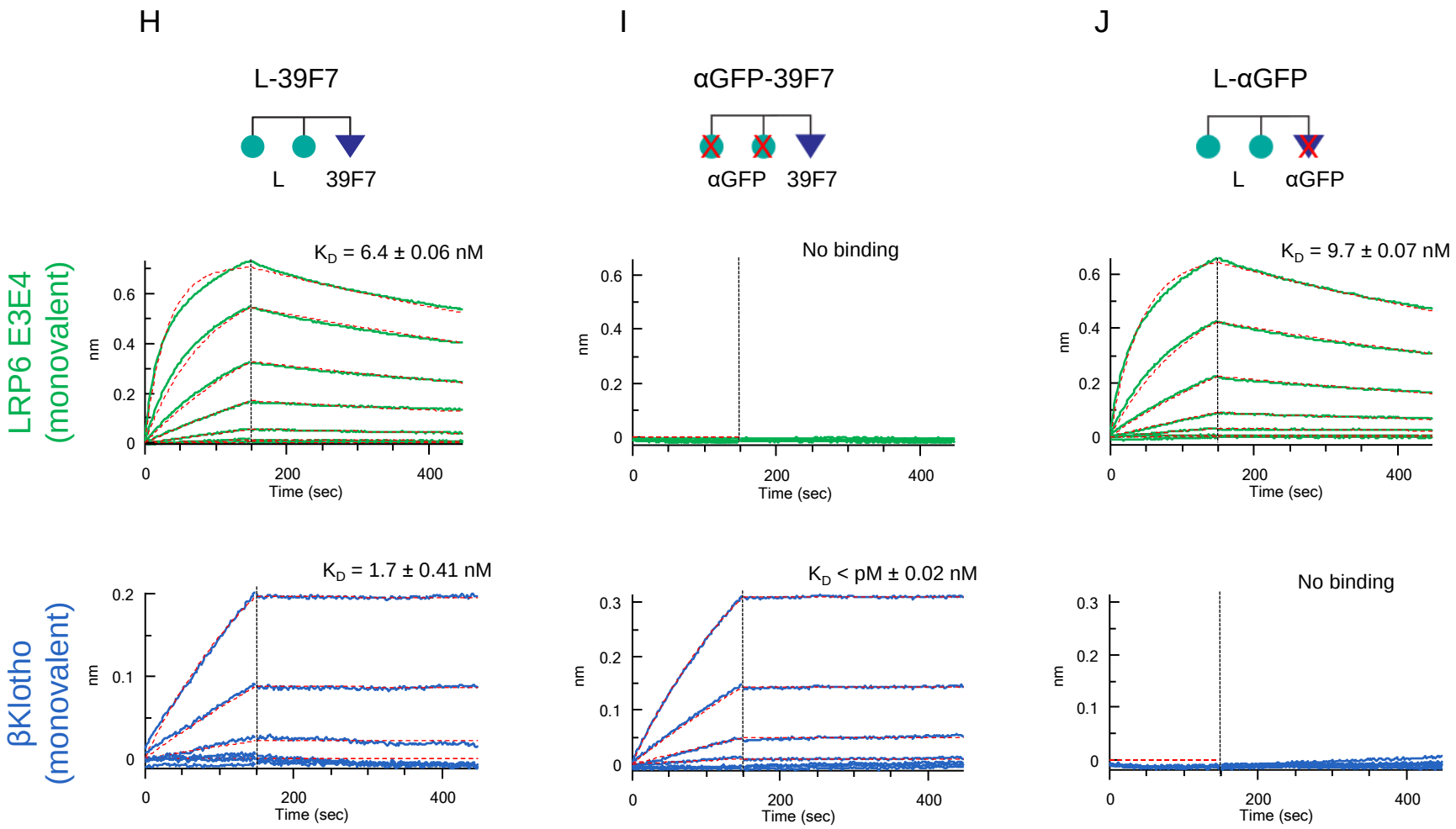
H
I
J
L-39F7
αGFP-39F7
L-αGFP
L
39F7
αGFP
39F7
L
αGFP
LRP6 E3E4 (monovalent)
βKlotho (monovalent)
K_D = 6.4 ± 0.06 nM
No binding
K_D = 9.7 ± 0.07 nM
K_D = 1.7 ± 0.41 nM
K_D < pM ± 0.02 nM
No binding
nm
Time (sec)

Figure 2

K

F-FGF21 series → FZD_7 → βKlotho

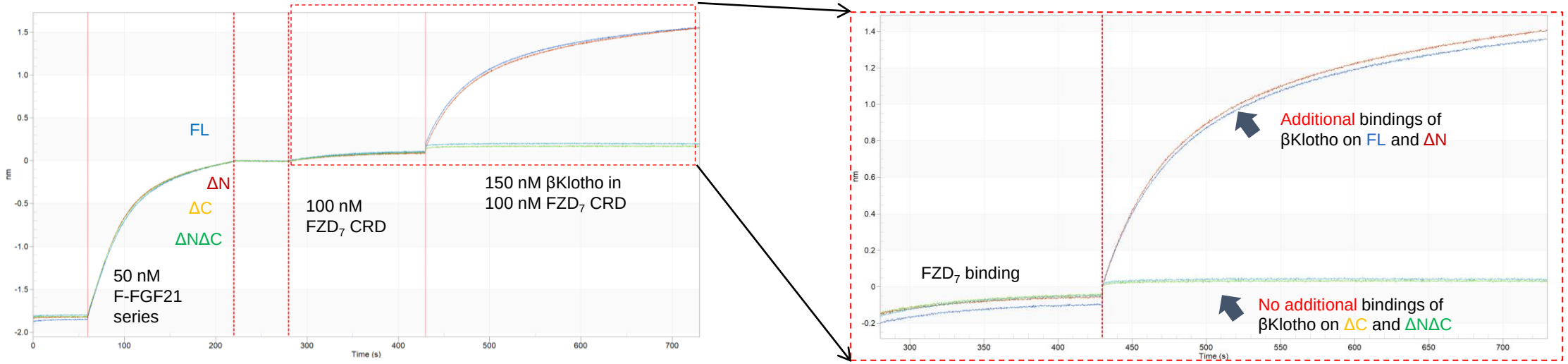

L

L-39F7 series → LRP6 → βKlotho

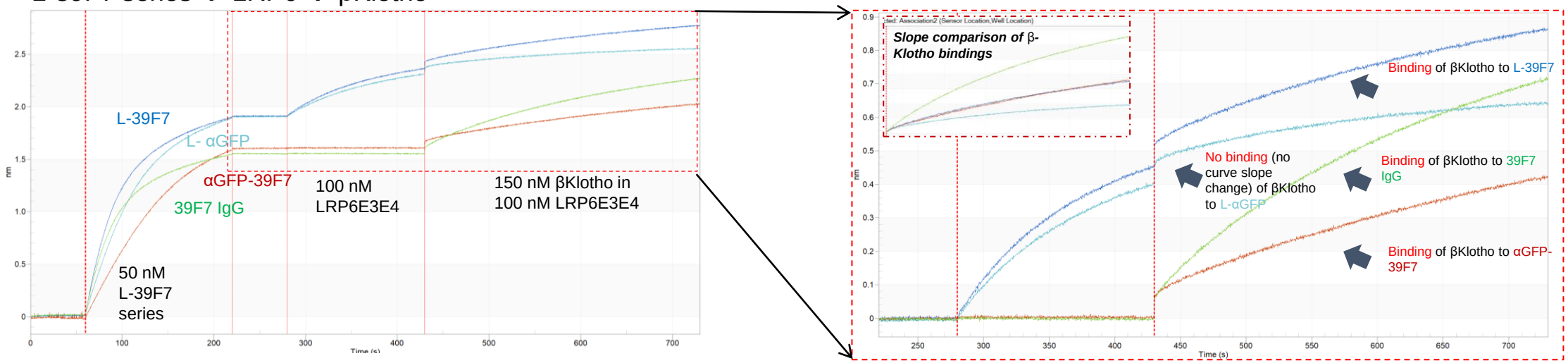

Figure 3

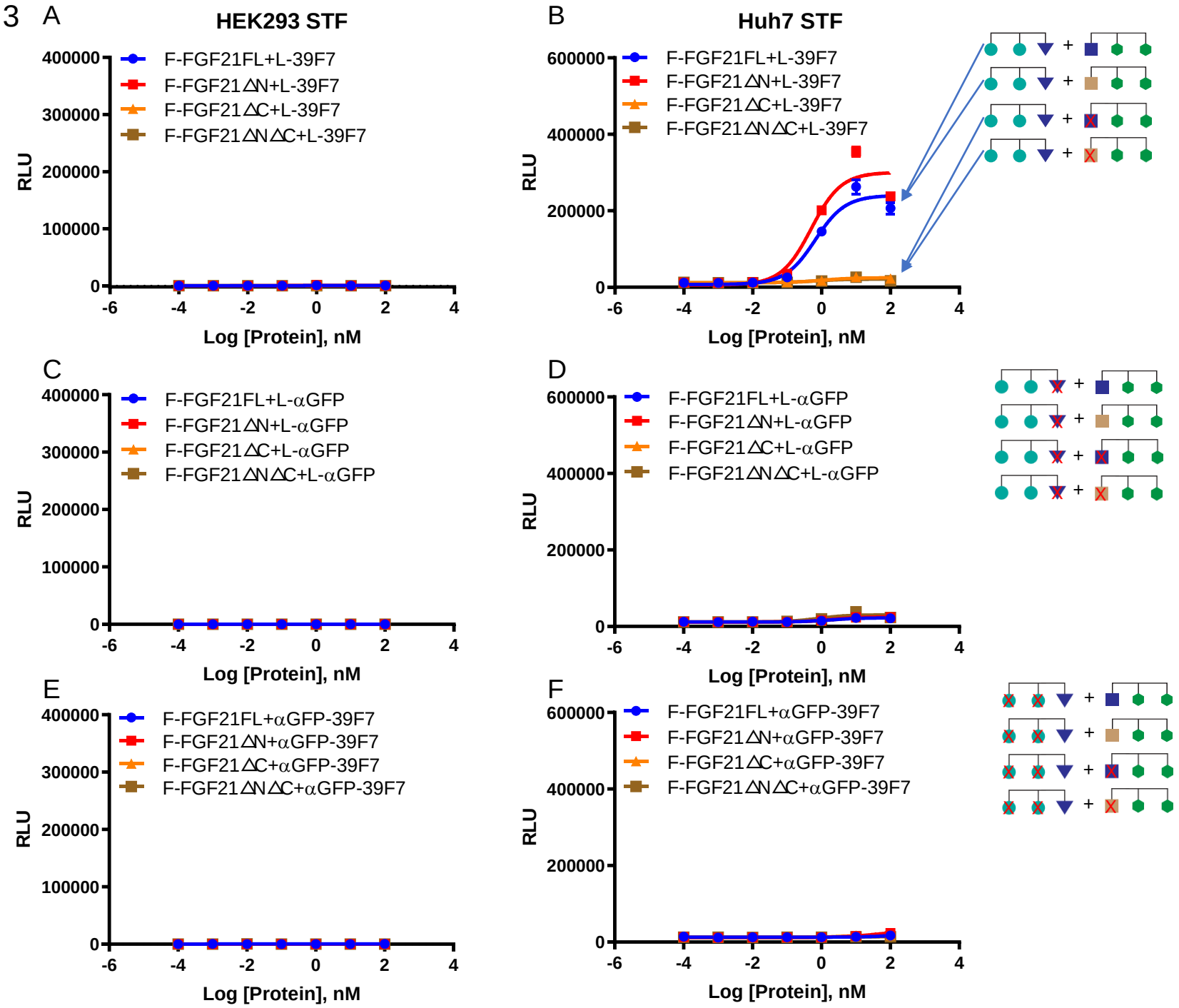
A
HEK293 STF
F-FGF21FL+L-39F7
F-FGF21ΔN+L-39F7
F-FGF21ΔC+L-39F7
F-FGF21ΔNΔC+L-39F7
RLU
Log [Protein], nM
B
Huh7 STF
C
F-FGF21FL+L-αGFP
F-FGF21ΔN+L-αGFP
F-FGF21ΔC+L-αGFP
F-FGF21ΔNΔC+L-αGFP
D
E
F-FGF21FL+αGFP-39F7
F-FGF21ΔN+αGFP-39F7
F-FGF21ΔC+αGFP-39F7
F-FGF21ΔNΔC+αGFP-39F7
F

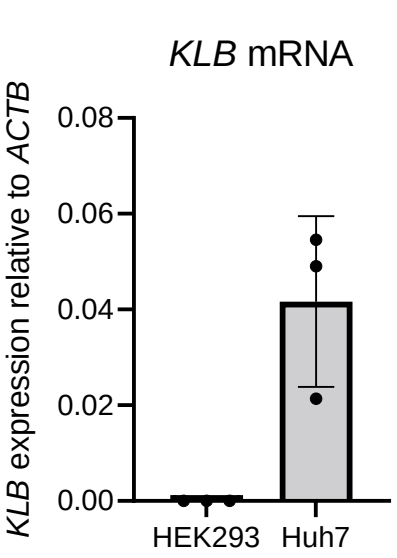
G
KLB mRNA
KLB expression relative to ACTB
HEK293
Huh7

Figure 4

A

Primary human hepatocytes

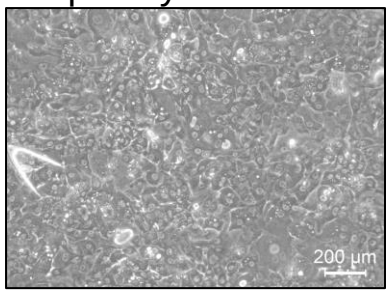

Human small intestinal organoids

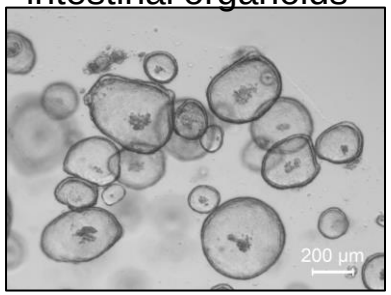

B

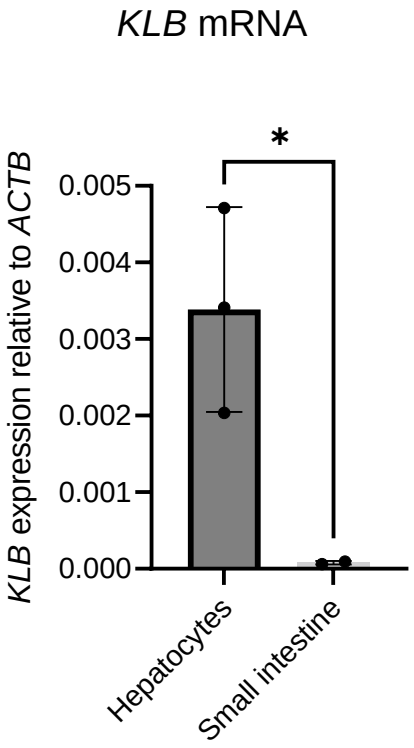

C

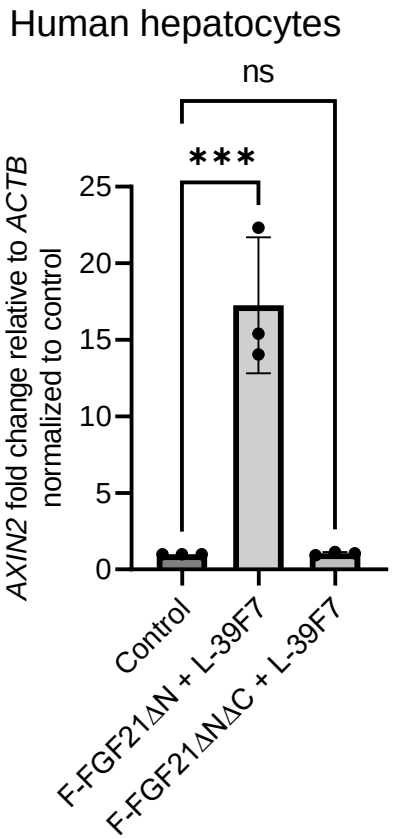
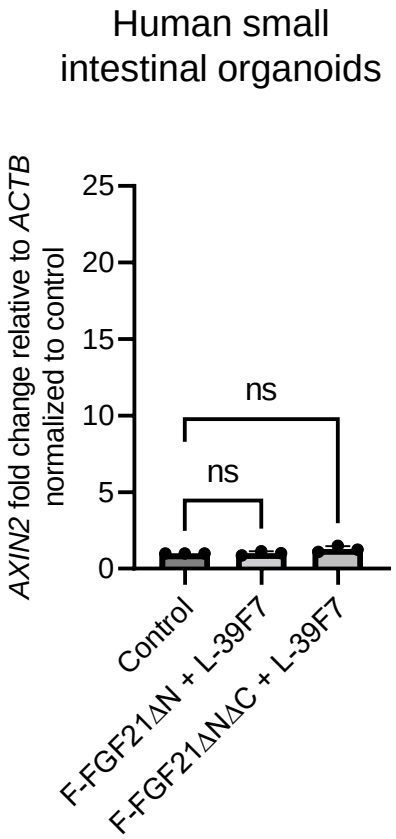
D